

PHOTOIONIZATION OF CIRCUMSTELLAR DISCS

Richard Alexander, Cathie Clarke & Jim Pringle
*Institute of Astronomy, Madingley Road
Cambridge, CB3 0HA, UK*



Models of discs around low-mass stars which couple photoevaporative mass-loss with viscous evolution have recently become important, as they are able to reproduce a number of observed disc properties successfully. However these models are subject to few observational constraints, and a number of issues remain unresolved and/or unexplored. In particular, the origin of the ionizing radiation required to drive the photoevaporation is not well-understood. In this contribution we review existing photoionization models, before going on to discuss recent and current work. Theoretical models of the accretion shock are considered, and we suggest a new observational diagnostic to quantify the chromospheric ionizing flux. We also consider the effects of X-ray photoionization in these models. We conclude that accretion powered UV and coronal X-rays are unlikely to influence disc evolution significantly. However the chromospheric Lyman continuum appears to be sufficient to drive disc photoevaporation, and so these models may indeed provide a realistic mechanism for dispersing circumstellar discs.

Keywords: accretion, accretion discs – stars: formation – circumstellar matter – planetary systems: protoplanetary discs – stars: pre-main sequence

1 Introduction

The existence of discs around young low-mass stars is now well established, and remains an important area of study as it has strong consequences for theories of both star and planet formation. Observations show us that at an age of $\sim 10^6$ yr most low-mass stars are surrounded by discs that are optically thick to optical and near-infrared radiation (Kenyon & Hartmann 1995³¹; Haisch et al. 2001²⁴; Lada & Lada 2003³⁴). These discs typically have masses of a few percent of a stellar mass (Beckwith et al. 1990⁶) and are much more massive than the low-mass “debris discs” observed in older systems (Mannings & Sargent 1997³⁷). By an age of $\sim 10^7$ yr, however, almost all of the discs have gone, and so this constrains the disc lifetimes to be of order

a few million years. There is also evidence for an intrinsic spread in these disc lifetimes of up to an order of magnitude (Armitage et al. 2003⁵).

However it is also well-established that the fraction of so-called transition objects, between disc-bearing Classical T Tauri stars and disc-less (or at least “optically thick disc-less”) Weak-lined T Tauri stars (hereafter CTTS and WTTS), is small. This has been observed by a number of near-infrared studies (eg. Skrutskie et al. 1990⁴⁶; Kenyon & Hartmann 1995³¹), and the effect has also been observed at mid-infrared (eg. Persi et al. 2000⁴¹; Bontemps et al. 2001⁷) and millimetre wavelengths (Simon & Prato 1995⁴⁵; Wolk & Walter 1996⁴⁷; Duvert et al. 2000¹⁴). This constrains the transition time between the CTTS and WTTS to be $\sim 10^5$ yr, with the disc vanishing simultaneously on spatial scales from 0.1-100AU on a timescale some 1-2 orders of magnitude shorter than the disc lifetime^a. This effect is observed most clearly in low-mass star-forming regions such as Taurus-Auriga and ρ Ophiuchus, and so it seems likely that the mechanism responsible is something intrinsic to individual TTS systems rather than an environmental effect. However most mechanisms for disc clearing, such as viscous evolution (Hartmann et al. 1998²⁶) or magnetospheric clearing (Armitage et al. 1999⁴), produce power-law declines in the disc surface density. Thus such models always produce a disc dispersal time that is comparable to the disc lifetime, and so fail to satisfy the two-timescale constraint required by the observations. Further, the simultaneous decline in the disc surface density observed across such a wide range of radii implies that the formation of a planet is unlikely to be responsible for this effect, as it is questionable whether a planet can account for such global changes in the disc properties.

One model which has been successful in reproducing the observed rapid disc dispersal times is the “UV switch” model of Clarke et al. (2001)¹¹. This model couples a photoevaporative disc wind to viscous evolution of the disc, and results in a rapid decline in the inner disc at a late stage in the disc evolution. Models of photoevaporative disc winds were first produced by Hollenbach et al. (1994)²⁷, and were subsequently improved upon by a number of subsequent studies (eg. Richling & Yorke 1997⁴³; Font et al. 2004¹⁷; see also the review by Hollenbach et al. 2000²⁸). In these models ultraviolet photons from the central star produce a thin, ionized layer on the disc surface, at a temperature of $\sim 10^4$ K. Outside some gravitational radius (~ 10 AU for a $1M_{\odot}$ star) the thermal energy of this ionized layer is such that it is greater than the gravitational binding energy, and so material can flow from the disc as a “disc wind”. The mass-loss rate is low, typically of order $10^{-10}M_{\odot}\text{yr}^{-1}$, and depends only on the mass of the central object and the ionizing flux, with the mass-loss concentrated at or near to the gravitational radius. When these models are coupled to a model including viscous evolution of the disc the results at early times are the same as for a ordinary viscous evolution model. However at late times the mass accretion rate through the disc drops to a value comparable to the disc wind mass-loss rate. At this point the inner disc cannot be resupplied with material inside the gravitational radius, and so the inner disc drains on a viscous timescale. Thus after a disc lifetime of $\sim 10^7$ yr the inner disc is dispersed on a timescale of $\sim 10^5$ yr, satisfying the two-timescale constraint demanded by observations (Clarke et al. 2001¹¹).

However a number of problems and caveats still exist in this model, which we seek to address in this contribution. The primary uncertainty surrounds the ionizing flux produced by the central object. In order to succeed this model requires an ionizing flux on the order of 10^{40} – 10^{43} photons s^{-1} , some ten orders of magnitude greater than that produced by a typical stellar photosphere. Further, this ionizing flux must be present at late times in the disc evolution, and

^aThis rapid dispersal is most clearly observed in the near-infrared. This near-infrared emission is due to warm dust in the disc, so it is only necessarily the *dust* which must disperse on this short timescale to satisfy the observations. However millimetre observations, which probe the gas in the disc, also show evidence for this rapid transition, and a strong correlation has been observed between the gas and dust emission (Najita et al. 2003³⁹), so we treat the gas and dust dispersal as simultaneous.

so ideally should not be powered by disc accretion. This problem is essentially unconstrained by observations, and so we investigate the production of Lyman continuum photons both by the accretion shock (Section 2) and the stellar chromosphere (Section 3). In contrast to the case of Lyman continuum photons, X-rays from TTS are well-studied, with typical luminosities of order $10^{30} \text{erg s}^{-1}$ (Feigelson & Montmerle 1999¹⁵). Such energies are similar to that produced by the Lyman continuum, and so in Section 4 we consider whether this X-ray emission could also drive a disc wind. We do not yet address the other main problem with the model, that the outer disc, beyond the gravitational radius, is dispersed more slowly than demanded by observations (Clarke et al. 2001¹¹). In essence this contribution summarises the work of three papers in turn (Alexander et al. 2004a¹; 2004b²; 2004c³), before bringing the separate conclusions together in a single summary.

2 Ionizing photons from the accretion shock

One possible source of Lyman continuum photons from TTS is from the “accretion shock” produced where disc materials falls onto the stellar surface. Discs around TTS are typically truncated by the magnetosphere at radii of $5\text{--}10R_*$ (eg. Calvet & Gullbring 1998¹⁰), and so material falling from the inner edge of the disc can attain extremely high velocities, of order $\sim 100 \text{km s}^{-1}$. This infalling material is channeled by the stellar magnetosphere and results in a so-called “accretion shock” where it impacts on the stellar surface. Existing models of the accretion shock (eg. Calvet & Gullbring 1998¹⁰; Gullbring et al. 2000²³) have primarily focused on reproducing spectra observed at ultraviolet ($1000\text{--}3000\text{\AA}$) and visible ($3500\text{--}7000\text{\AA}$) wavelengths, and such emission spectra are now well understood. However absorption by interstellar H I makes observations at wavelengths shortward of the Lyman break ($< 912\text{\AA}$) impossible, and so little is known about the Lyman continuum emission produced by the accretion shock. Observations indicate that the accretion shock has a typical temperature of $10,000\text{--}15,000\text{K}$ (eg. Johns-Krull et al. 2000³⁰), and so previous studies have estimated the ionizing flux produced by the accretion shock by assuming that the accretion shock emits like a black body “hotspot” on the stellar surface (Matsuyama et al. 2003³⁸). We contend that the ionizing flux produced by such a hotspot will be greatly suppressed, for two reasons. Firstly, the hotspot itself is likely to radiate like a heated stellar atmosphere rather than a simple black body, and in such a case photoionization of neutral hydrogen results in a strong “Lyman edge” in the spectrum at the Lyman break. Further, any ionizing photons produced by the hotspot must travel upwards through the accretion column in order to escape and ionize the disc surface. The accretion column is extremely optically thick to Lyman continuum photons due to its high density of H I, and so this provides an extremely strong suppression of the ionizing flux. We address each of these issues in turn.

2.1 Stellar Atmospheres

Previous studies (eg. Matsuyama et al. 2003³⁸) have assumed that the accretion shock can be modelled as a constant temperature hotspot, with the spectral energy distribution (SED) of the hotspot that of a $T = 15,000\text{K}$ blackbody. Half of the accretion energy is assumed to be radiated by the hotspot, and so for a star of mass M_* and radius R_* the accretion luminosity is given by

$$L = \frac{GM_*\dot{M}_d}{2R_*} = A\sigma_{SB}T^4 \quad (1)$$

where \dot{M}_d is the rate of mass accretion from the disc, A is the area of the hotspot, and σ_{SB} is the Stefan-Boltzmann constant. As the temperature is constant, the ionising photon rate Φ_a is proportional to the accretion rate \dot{M}_d . Matsuyama et al. (2003)³⁸ also include a photospheric

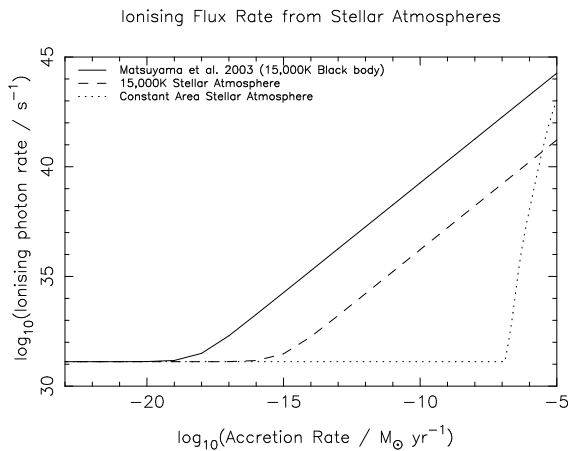


Figure 1: Ionising flux rates from different accretion shock models. The rate from a simple model atmosphere is some 3 orders of magnitude less than that from a blackbody, and the constant area case, with $T \propto \dot{M}_d^{1/4}$ decays more precipitously still. (Figure from Alexander et al. 2004a¹.)

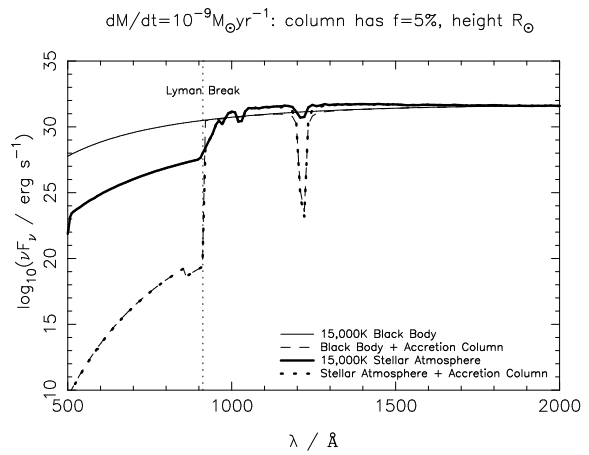


Figure 2: Spectra of light incident on and emitted by a constant density accretion column with a covering factor of 5% and a height of $1R_\odot$. Note the precipitous drop in the emitted spectra at the Lyman break, due to photoabsorption by H α . The deep absorption feature at 1215\AA is Ly α . (Figure from Alexander et al. 2004a¹.)

contribution to the ionizing flux of $\Phi_p = 1.29 \times 10^{31} \text{ photon s}^{-1}$, with the total ionizing flux given by $\Phi_a + \Phi_p$.

We propose two corrections to this model. Firstly, we assert that the high density of atomic hydrogen in the accretion shock will result in a SED that more closely matches that of a stellar atmosphere, showing a significant Lyman edge at 912\AA . By repeating the calculation above, but this time adopting the SED of a 15,000K Kurucz stellar atmosphere (Kurucz 1992³³), we find that the ionizing flux from a 15,000K hotspot is reduced by 3 orders of magnitude. The second correction concerns the hotspot area. The formulation in Equation 1 uses a constant temperature, thus implying that the hotspot area decreases as the accretion rate drops. However if the accretion onto the stellar surface is channeled by the magnetosphere then the hotspot area should remain approximately constant with time. If the area of the blackbody hotspot A is indeed constant, then it is clear from Equation 1 that the hotspot temperature should vary as $T \propto \dot{M}_d^{1/4}$. As the *total* luminosity of the stellar atmosphere is very similar to that of a blackbody we adopted this criterion also. We then re-evaluate the ionizing flux from the hotspot as before, again keeping the scaling luminosity proportional to \dot{M}_d , but this time with the hotspot temperature given by

$$T = \left(\frac{GM_*}{2R_* A \sigma_{SB}} \dot{M}_d \right)^{1/4} \quad (2)$$

The results of both of these models are shown in Fig.1, with the blackbody result assumed by Matsuyama et al. (2003)³⁸ shown for comparison. In the case of constant area the fall in ionizing flux with accretion rate is much more dramatic than in the constant temperature case, with only high accretion rates ($> 10^{-7} M_\odot \text{ yr}^{-1}$) producing ionizing photons at greater than the photospheric rate. The relationship between hotspot area and accretion rate is not well understood, with some evidence even suggesting an area that increases with \dot{M}_d (Calvet & Gullbring 1998¹⁰). However we go on to show that the presence of the accretion column above the hotspot is the dominant factor in determining Φ_a , and so the exact details of the hotspot area are not of great significance.

2.2 Accretion Columns

The other issue we consider is the presence of a column of accreting material directly above the hotspot. This accretion column absorbs Lyman continuum photons through photoionization of neutral hydrogen, and so the ionizing flux is greatly suppressed. The photoionization cross-section for absorption of Lyman continuum photons is $\sigma_{13.6\text{eV}} = 6.3 \times 10^{-18} \text{cm}^2$, and so a column density of $1.58 \times 10^{17} \text{cm}^{-2}$ is equivalent to an optical depth of unity. The density of the infalling material is of order 10^{12}cm^{-3} (Calvet & Gullbring 1998¹⁰), and so the typical attenuation length is of order $10^{-5} R_{\odot}$. Thus all Lyman continuum photons from the accretion shock are absorbed by the column, and the only significant source of ionizing photons that can escape the column is radiative recombination within the column, the so-called diffuse continuum.

In order to study the diffuse continuum we constructed models of the accretion column using the photoionization code CLOUDY (Ferland 1996¹⁶). Our model uses the hotspots described above as a source, placed beneath a column which subtends a constant solid angle (ie. the column is a truncated radial cone). We assume a magnetospheric accretion model (eg. Ghosh & Lamb 1978¹⁸), with the density of the column scaling as $R^{-5/2}$, and follow the parametrization of Calvet & Gullbring (1998)¹⁰ in fixing the scaling density at the base of the column. As the diffuse continuum dominates, the ionizing flux emitted by the column is insensitive to the exact input SED and so the blackbody and stellar atmosphere hotspots both give the same diffuse Lyman continuum, as seen in Fig. 2. We compute these models for a broad range of accretion rates, column heights and covering fractions, and find that in all cases the flux emitted from the top of the column was much less than the photospheric level (a typical spectrum is shown in Fig. 2).

2.3 Discussion

The most obvious caveat in our model is that we only consider radial photons, and neglect emission from the “sides” of the columns. Given the enormous optical depth only a negligible fraction of the ionizing photons emitted near to the edge of the hotspot can escape. However the diffuse continuum emitted from the sides of the column is significant, and in fact is probably dominant. Given that this emission should be isotropic we can evaluate its value approximately by considering a column with a height equal to its diameter: in all cases the ionizing flux emitted is still less than the photospheric value. We also neglect both flaring and bending of the accretion column, but the uncertainties due to these effects are small. Even our “best-case” model, with parameters chosen so as to maximise the ionizing flux, fails to produce Lyman continuum photons at greater than the photospheric rate. The photospheric rate of $1.29 \times 10^{31} \text{photon s}^{-1}$ is some 10 orders of magnitude less than the value required to drive disc photoevaporation in the models described in Section 1, and so we conclude that the accretion shock does not produce Lyman continuum photons at a rate likely to be significant in these models. Therefore, in order for photoevaporation to be a realistic means of disc dispersal the central source must sustain a source of ionizing photons that is not powered by disc accretion.

3 Ionizing photons from the chromosphere

A second possible source of Lyman continuum photons from TTS is the stellar chromosphere. Chromospheric emission from young stars is poorly understood, and no real constraints exist on the ionizing flux produced. However these stars are known to be magnetically active, and so some authors have argued that a chromosphere that resembles a “scaled-up” solar chromosphere seems likely (eg Costa et al. 2000¹²). The rate of Lyman continuum photons from the solar chromosphere is $\sim 10^{38} \text{photon s}^{-1}$, and so a scaled up value would approach the rates required by photoevaporation models. However, as stressed by Clarke et al. (2001)¹¹, in addition to a strong

ionizing flux merely being present around TTS, in order to drive the photoevaporation it must remain present at late times in the disc evolution. Thus we seek to place observational constraints on the chromospheric Lyman continuum emitted by TTS, both in terms of its magnitude and evolution.

There are, however, a number of observational issues that make this difficult. Most obviously, Lyman continuum photons are absorbed by interstellar H I and so direct measurements of the ionizing flux are not possible. Hydrogen recombination lines are of limited use as a diagnostic, as they are invariably optically thick. They also suffer from the fact that it is difficult to separate the disc emission from that from the central source. Further, even when a diagnostic is found reddening is a significant problem, as small uncertainties in the extinction and reddening law at optical wavelengths result in much larger uncertainties when extrapolated to the ultraviolet.

In order to address this we make use of two techniques. Firstly, we use an emission measure (EM) analysis. In plasma physics, the EM is a measure of the mass of material emitting at a given temperature, and so combining the EM with a spectral synthesis package leads directly to a predicted spectrum. By assuming that the chromosphere around these objects radiates as an optically thin plasma, Brooks et al. (2001)⁸ were able to derive volume emission measures for a sample of 5 CTTS. By utilising these EMs (kindly provided by David Brooks) we are able to derive reddening-dependent values of the ionizing flux emitted by these objects.

Secondly, we make use of the result noted by Brooks & Costa (2003)⁹ that the total power radiated by the chromosphere is observed to correlate well with the flux in the C IV 1549Å doublet. We also note that the He II 1640Å line is the equivalent of H α for singly-ionized He, and is thought to be excited by radiative recombination. Thus the flux in the He II line should provide an indicator of the ionizing flux present, and the He II :C IV line ratio should provide a reddening-independent, normalised diagnostic. We then use archival (IUE) data to obtain He II :C IV ratios for ~ 40 TTS, both classical and weak-lined, in order to study the time evolution of the ionizing flux.

3.1 Emission Measures

In order to perform our EM analysis we make use of the EMs derived by Brooks et al. (2001)⁸. We use these EMs as input for the CHIANTI spectral synthesis code (Dere et al. 1997¹³), and adopt the stellar parameters of Brooks & Costa (2003)⁹. We first attempt to reproduce the observed spectra, and find that the line ratios and intensities can generally be reproduced to within a factor of $\simeq 2$ of the observed values. (We note, however, that none of the synthetic spectra contain significant He II 1640Å emission, in contrast to the observations. The plasma simulation only includes collisional excitation, and so we interpret this as evidence that the He II 1640Å line is excited by radiative recombination.) We then use the synthetic SEDs to estimate the ionizing fluxes produced by these TTS. These values are obviously subject to large reddening uncertainties, and so are probably only accurate to order-of-magnitude level, but indicate that the ionizing fluxes fall in the range 10^{41} – 10^{43} photon s^{-1} .

3.2 He II :C IV Line Ratio

We also study the behaviour of the He II :C IV line ratio, comparing the observed line ratios to the ratios of ionizing flux to total chromospheric power derived from the EM analysis above. The sample is small (5 objects), but it does indicate that a strong correlation between these two quantities, supporting the hypothesis that the line ratio is a useful diagnostic of the ionizing flux. In essence the ratio is a “hardness ratio”, with a smaller value of the line ratio being indicative of a softer ionizing spectrum.

In order to study the evolution of the ionizing flux with time, we have made use of the data from the IUE final archive (Johns-Krull et al. 2000³⁰). From this we were able to obtain

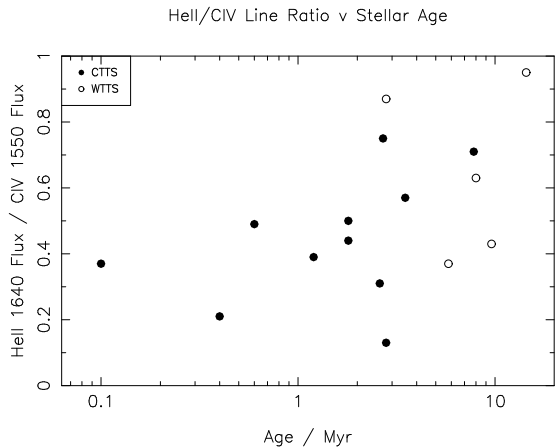


Figure 3: Plot of line ratio versus stellar age, with ages taken from Palla & Stahler (2002)⁴⁰. The ratio stays approximately constant with age, as it does with all evolutionary indicators, and the highest values are from WTTS. (Figure from Alexander et al. 2004c³.)

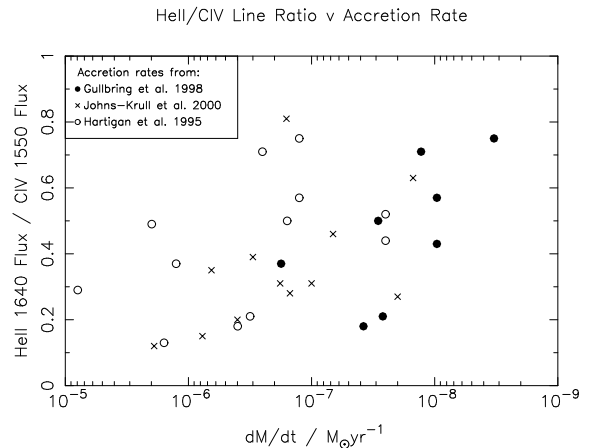


Figure 4: Plot of line ratio versus mass accretion rate, with objects “evolving” to the right. Three different sources are used for the accretion rates, each with their own different systematics, but the trend remains the same. (Figure adapted from Alexander et al. 2004c³.)

HeII:CIV ratios for ~ 40 sources. We then plot these line ratios against a number of evolutionary indicators, where such data exist (ie. mass accretion rate, stellar age, $H\alpha$ equivalent width: see Figs.3 & 4). There is significant scatter in the data and the number statistics are unfavourable, but the general trends all show that the line ratio stays approximately constant against each age indicator, and if anything actually increases as the objects evolve. In addition, the highest values of the line ratio tend to come from WTTS, indicating that evolved systems do produce strong ionizing fluxes. The results show no dependence on other parameters (stellar M/R ratio, spectral type), and so we conclude that the ionizing flux produced by the chromosphere of TTS shows no evidence of any significant decline over the lifetime of the TTS phase of evolution.

3.3 Discussion

Our analysis is obviously crude, but given the lack of any existing observational constraints on this problem it does provide a valuable new insight. The dominant uncertainty in the ionizing flux values determined are due to reddening, and these are much greater than the uncertainties due to other potential sources of error. Thus we consider our order-of-magnitude estimates of 10^{41} – 10^{43} photon s^{-1} to be plausible.

With regard to the line ratio, the dominant uncertainties lie in the use of the HeII 1640Å line. Firstly, the ionization energy for HeII is 54.4eV, and so the recombination lines only really give an indicator as to the presence of flux at wavelengths $< 228\text{\AA}$, rather than 912\AA . Thus we do not probe the region from 228\AA – 912\AA directly. However it is difficult to envisage an emission mechanism which could produce photons in this spectra range without producing higher energy photons also, and so the HeII recombination lines should provide a reasonable indicator of the ionizing flux.

There is also the question of whether the HeII emission comes from radiative recombination or is due to collisional excitation. Studies of the solar corona show that both mechanisms play a role, and studies of the chromospheres of nearby bright stars have found similar results (eg. Linsky et al. 1995³⁵, 1998³⁶). High resolution spectroscopy can be used to distinguish the two processes, as they result in very different line profiles, but unreasonably long exposure times are necessary when observing TTS (around 50 hours per source with HST!). However any plasma hot enough to produce significant collisional population of the $n = 3$ state of HeII (48.4eV above the ground state) would be expected to radiate significantly at wavelengths $> 912\text{\AA}$ through

free-free radiation and bound-free transitions, and so the presence of strong HeII 1640Å emission should be a reliable indicator as to the presence of a strong ionizing flux in both cases. Also, the absence of HeII 1640Å emission in the synthetic spectra derived from the EMs (which do not consider photo-excitation) supports the radiative recombination hypothesis. Other uncertainties, such as possible opacity in the CIV 1549Å line, are less significant than those discussed here.

The last potential problem regards getting the ionizing photons to the disc. We have already seen that the accretion shock is extremely optically thick to Lyman continuum photons, and the outflow/jet from the central source may be optically thick also (Shang et al. 2002⁴⁴). Thus it may be that chromospheric ionizing photons are absorbed before they can reach the disc. The location of the chromospheric emission is not well-established, however, and so this question remains open.

We have shown that TTS chromospheres do indeed seem to produce ionizing photons at a rate large enough to be significant in photoevaporation models, with ionizing fluxes in the range 10^{41} – 10^{43} photon s^{-1} . Moreover we propose that the HeII:CIV line ratio may act as a diagnostic of the ionizing flux, and by studying archival data we find that the ionizing flux remains approximately constant as objects evolve. Thus chromospheric emission can be sufficient to drive disc photoevaporation, as required by the model of Clarke et al. (2001)¹¹.

4 X-ray driven disc winds?

A further possible source of disc heating is X-rays. Both CTTS and WTTS are known to be strong X-ray sources, with typical X-ray luminosities on the order of 10^{28} – 10^{30} erg s^{-1} (eg. Feigelson & Montmerle 1999¹⁵). Previous studies of the X-ray/disc interaction have focused primarily on using X-rays to sustain the low levels of ionization required to drive the magnetorotational instability (Glassgold et al. 1997²⁰; Igea & Glassgold 1999²⁹), or looked at the effect of X-ray heating on the observed spectrum (Glassgold & Najita 2001¹⁹; Gorti & Hollenbach 2004²²). However they have not considered the potential this interaction has to drive a disc wind: here we make a preliminary study into the significance of this effect.

When soft X-rays, of the type emitted by TTS, are incident on a circumstellar disc a number of processes occur. These are discussed in great detail by Krolik & Kallman (1983)³² (see also Glassgold et al. 2000²¹); here we merely provide a short summary of the relevant points. The incident X-ray photons are absorbed by heavy elements (typically O or C, with some Fe absorption also). A single photoelectron is produced, with an energy essentially equal to that of the incident photon. This “primary” electron then collides with neutral hydrogen or helium in the gas, generating a large number (~ 30) of “secondary” electrons. This process accounts for the majority of the ionization, and thus heating, in our models. Collisional charge exchange between ionized heavy species and light neutrals accounts for a few percent of the total heating, and the Auger effect (2-electron decay) is negligible. In addition, we note that the probability of a diffuse X-ray field is very small, as recombinations producing X-rays are rare. Thus all the heating is along the line-of-sight - a significant difference from the UV case. Throughout the following modelling we assume solar gas composition, and adopt model parameters of $M_* = 1M_\odot$ (stellar mass) and $M_d = 0.01M_\odot$ (disc mass).

4.1 Basic Model

As a first iteration we construct a simple 1-dimensional model. Here we make the approximation that the disc can be divided into a series of concentric, non-interacting annuli. We adopt an initial steady disc model, with the disc surface density given by a R^{-1} power-law (eg. Beckwith

et al. 1990⁶) and the disc temperature given by

$$T(R) = \left(\frac{R}{1AU} \right)^{-1/2} 100\text{K} \quad (3)$$

Thus, by solving the equation of hydrostatic equilibrium, we can show that at each radius R the vertical structure of the disc is given by a Gaussian density profile (Pringle 1981⁴²) with a scale height

$$H(R) = \left(\frac{c_s^2 R^3}{GM_*} \right)^{1/2} \quad (4)$$

where c_s is the local isothermal sound speed.

We take our initial disc structure and, using the CLOUDY photoionization code, study what happens at each radius R when the disc is irradiated from above by X-rays. We adopt an X-ray source position of $R = 0$, $z_s = 10R_\odot$, a source luminosity of $L_X = 10^{30}\text{erg s}^{-1}$, and take the source spectrum to be that of 10^7K bremsstrahlung (typical of that observed in TTS). Thus we evaluate the flux, F_X , downwardly incident on each annulus as

$$F_X = \frac{L_X}{4\pi R^2} \frac{z_s}{\sqrt{R^2 + z_s^2}} \quad (5)$$

where the first term represents simple geometric dilution of the energy, and the second the sine of the incidence angle. For a given density structure CLOUDY returns a temperature profile $T(z)$. Thus by solving the equation of hydrostatic equilibrium in the non-isothermal case at each radius R we generate a new density profile and are able to iterate towards a self-consistent structure. The results of this procedure at $R = 10R_\odot$ are shown in Fig.5. Above some reference point, the temperature rises gradually to around 10,000K. In order to heat to higher temperatures than this the disc material must be mostly ionized, and so only the very low density upper regions of the disc are heated to $>10,000\text{K}$. The density structure is actually well-fit by a two-temperature structure, with a best-fit temperature of 6200K in the upper region. However this 1D model breaks down at radii $\gtrsim 30R_\odot$, as the disc expands to a height comparable to the source height, and so the approximation of downward incidence (Equation 5) is no longer valid. Thus we must construct a 2-dimensional model in order to study the behaviour at larger radii.

4.2 2D Model

We extend the model to consider a simple 2D case as follows. As the vertical structure of the disc is well-modelled by the two-temperature profile described above, the critical factor in determining the overall structure of the disc is the location of the transition point between the heated and cold regions. This in turn is determined by how far the X-rays penetrate into the disc. Thus we can solve for the location of the transition point we can determine the effects of the X-ray heating.

The X-rays penetrate the disc along the line-of-sight to a critical value of the parameter

$$\xi = \frac{L_X J_h}{n d^2} \quad (6)$$

where n is the local particle number density, d the distance along the line-of-sight to the source and where the factor J_h accounts for the attenuation of the flux due to absorption along the line-of-sight (Krolik & Kallman 1983³²). Essentially ξ represents the photon to particle density ratio at a given location. We evaluate the attenuation factor numerically by integrating the column along the line-of-sight, and then using the approximate parametrization for J_h derived by Glassgold et al. (1997)²⁰.

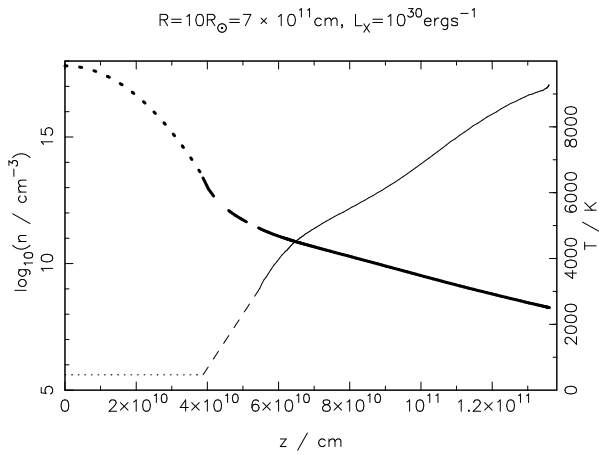


Figure 5: Density (heavy line) and temperature (lighter line) profiles evaluated by 1D model at a radius of $10R_{\odot}$. The solid region is calculated explicitly by the model, the dashed region is extrapolated, and the dotted region represents the isothermal midplane. The steepening of the $T(z)$ curve with decreasing z is due to the increased efficiency of 2-body cooling as the density increases. (Figure from Alexander et al. 2004b².)

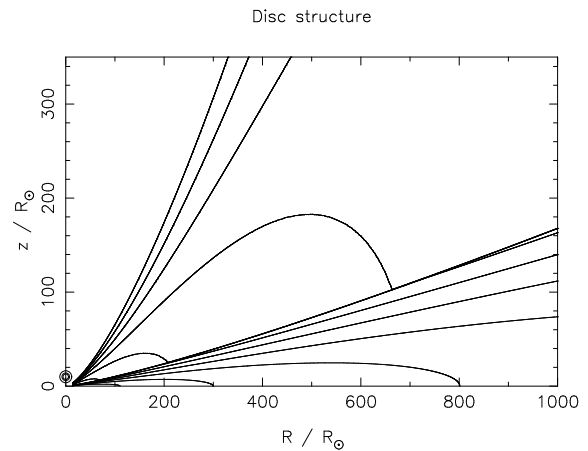


Figure 6: Structure of the X-ray heated disc evaluated by the 2D model. Density contours are drawn at $n = 10^{15}, 10^{14}, 10^{13} \dots 10^3 \text{ cm}^{-3}$. The location of the X-ray source at $R = 0, z_s = 10R_{\odot}$ is marked by circles. The transition point is clearly visible at the point where several contours are overlaid. Most of the X-ray attenuation occurs at $R \lesssim 100R_{\odot}$. (Figure from Alexander et al. 2004b².)

We use the inner disc structure obtained from our 1D model to produce a “starting” structure in the region $R = 10\text{--}20R_{\odot}$. From this we determine the critical value of the ionization parameter to be $\xi_c \simeq 10^{-8} \text{ erg cm s}^{-1}$. As the attenuation through the disc to a given radius R depends only on the disc structure at radii less than R , we can evaluate ξ at all values of z at this radius. The value which gives $\xi = \xi_c$ is adopted as the transition point for radius R , and so we can generate a vertical structure at R and iterate outwards through the disc. Thus we solve for the disc structure on a regularly-spaced (R, z) grid, with grid spacings of $2R_{\odot} = 1.39 \times 10^{11} \text{ cm}$ in R and 10^9 cm in z . Runs at higher resolution over a smaller spatial extent indicate that the numerical accuracy of this procedure is better than 10%. The disc structure obtained is shown in Fig.6.

We are able to make a crude estimate of the mass-loss that can be driven by X-rays by evaluating the mass-loss per unit area as ρc_s at the base of the heated column at the gravitational radius. The number density at the base of the column is $\simeq 10^5 \text{ cm}^{-3}$, which gives a value of for the mass-loss per unit area of $\simeq 10^{-13} \text{ g cm}^{-2} \text{ s}^{-1}$. This is comparable to the value for UV photoevaporation evaluated by Hollenbach et al. (1994)²⁷, who derive a value of $3.88 \times 10^{-13} \text{ g cm}^{-2} \text{ s}^{-1}$ for an ionizing flux of $10^{41} \text{ photons s}^{-1}$. However our value is to be regarded as an upper limit, for the reasons outlined below, and so we find that X-ray photoevaporation is at most comparable to UV photoevaporation, and almost certainly much less significant.

4.3 Discussion

There are a number of simplifications in our model, but two are of particular significance. Firstly, there is the manner in which we evaluate the vertical structure. The 2-temperature structure is adopted as it is a good fit to the results of the 1D model. However in the 1D model the CLOUDY code only solves explicitly for the structure at temperatures greater than 3000K (the code is not stable below this point). We assume that the temperature gradient is smooth at temperatures below this, and extrapolate down to the midplane temperature linearly (see Fig.5). This essentially puts the hot/cold transition point at as low a vertical position, and therefore as high a density, as the model permits. In reality it seems likely that there will be an extended

column of “warm” ($\sim 1000\text{K}$) material (eg. Glassgold & Najita 2001¹⁹; Gorti & Hollenbach 2004²²). In this case the hot temperatures required to drive mass-loss are only reached at higher z than in our model. As the density falls exponentially with z , even a relatively small warm column will significantly reduce the density at the base of the hot region, and so the “true” mass-loss rate will likely be significantly lower than that predicted by our model.

The other main simplification of our 2D model is the assumption of a constant temperature in the heated region. This is a best-fit, but tends to under-estimate the density at high z compared to the 1D models (as the temperature rises with increasing z). Most of the attenuation along the line-of-sight to the outer regions of the disc comes from material at radii $\lesssim 50R_{\odot}$, where the 1D approximation is still valid. By under-estimating the density at high z in this regions we in turn under-estimate the attenuation along the line-of-sight to the outer disc, and therefore in turn over-estimate the depth to which the X-rays penetrate the disc at larger radii. A more realistic temperature profile would therefore be expected to decrease the calculated mass-loss rate somewhat. A number of less significant approximations are also made, but are not discussed here for reasons of paper length.

Our 2D model is simplistic, and more realistic models are clearly needed to firm up our conclusion. However we are satisfied that our model represents a “best case” model, designed to maximise the mass-loss, and so we consider the derived mass-loss rate to be an upper limit. The true rate is most likely significantly lower. In the absence of any significant Lyman continuum flux an X-ray driven disc wind could be significant. However it seems that UV driven winds do exist, and so we do not consider it likely that X-ray driven disc winds are significant in dispersing circumstellar discs.

5 Summary

In this contribution we have reviewed models of disc photoevaporation, and considered several different means to resolve the major uncertainty with these models: the ionizing flux. We have shown that the accretion shock is unlikely to power disc photoevaporation, due to the extremely high optical depth of the accretion column. Similarly, it seems unlikely that X-rays can drive a significant disc wind, although more detailed calculations are needed to confirm this result. Studies of TTS chromospheres, however, seem to indicate that the chromosphere does produce a sufficient ionizing flux. Plasma modelling, using previously derived emission measures, indicate that the typical ionizing flux is in the range 10^{41} – 10^{43} photon s^{-1} , and by using the ultraviolet HeII:CIV line ratio as a hardness ratio we have shown that this flux is not expected to change significantly as the TTS evolve. Thus there does appear to be an ionizing flux sufficient to drive these models, and so they remain an interesting area of study.

Acknowledgments

RDA acknowledges the support of a PPARC PhD studentship, and also thanks the EC-RTN for supporting his attendance at this conference. CJC gratefully acknowledges support from the Leverhulme Trust in the form of a Philip Leverhulme Prize.

References

1. Alexander, R.D., Clarke C.J., Pringle, J.E., 2004a, MNRAS, 348, 879
2. Alexander, R.D., Clarke C.J., Pringle, J.E., 2004b, MNRAS submitted
3. Alexander, R.D., Clarke C.J., Pringle, J.E., 2004c, in preparation
4. Armitage, P.J., Clarke, C.J., Tout, C.A., 1999, MNRAS, 304, 425
5. Armitage P.J., Clarke C.J., Palla F., 2003, MNRAS, 342, 1139

6. Beckwith S.V.W., Sargent A.I., Chini R.S., Güsten R., 1990, AJ, 99, 924
7. Bontemps, S., André, P., Kaas, A.A. et al., 2001, A&A, 372, 173
8. Brooks, D.H., Costa, V.M., Lago, M.T.V.T., Lanzafame, A.C., 2001, MNRAS, 327, 177
9. Brooks, D.H., Costa, V.M., 2003, MNRAS, 339, 467
10. Calvet N., Gullbring E., 1998, ApJ, 509, 802
11. Clarke C.J., Gendrin A., Sotomayor M., 2001, MNRAS, 328, 485
12. Costa, V.M., Lago, M.T.V.T., Norci, L., Meurs, E.J.A., 2000, A&A, 354, 621
13. Dere, K.P., Landi, E., Mason, H.E., Monsignor Fossi, B.C., Young, P.R., 1997, A&AS, 125, 149
14. Duvert, G., Guilloteau, S., Ménard, F., Simon, M., Dutrey, A., 2000, A&A, 355, 165
15. Feigelson, E.D., Montmerle, T., 1999, ARA&A, 37, 363
16. Ferland G.J., 1996, *A Brief Introduction to CLOUDY*, University of Kentucky Department of Physics and Astronomy Internal Report
17. Font, A.S., McCarthy, I.G., Johnstone, D., Ballantyne, D.R., 2004, ApJ, 607, 890
18. Ghosh P., Lamb F.K., 1978, ApJ, 223, L83
19. Glassgold, A.E., Najita, J., 2001, in ASP Conference Series 244, 251
20. Glassgold, A.E., Najita, J., Igea, J., 1997, ApJ, 480, 344 (Erratum: ApJ, 485, 920)
21. Glassgold, A.E., Feigelson, E.D., Montmerle, T., 2000, in Mannings, V., Boss. A.P., Russell, S.S., eds, Protostars & Planets IV. Univ. Arizona Press, Tuscon, p. 429
22. Gorti, U., Hollenbach, D., 2004, ApJ in press (astro-ph/0405244)
23. Gullbring E., Calvet N., Muzerolle J., Hartmann L., 2000, ApJ, 544, 927
24. Haisch K.E., Lada E.A., Lada C.J., 2001, ApJ, 553, L153
25. Hartigan, P., Edwards, S., Ghandour, L., 1995, ApJ, 452, 736
26. Hartmann L., Calvet N., Gullbring E., D'Alessio P., 1998, ApJ, 495, 385
27. Hollenbach D., Johnstone D., Lizano S., Shu F., 1994, ApJ, 428, 654
28. Hollenbach, D.J., Yorke, H.W., Johnstone, D., 2000, in Mannings, V., Boss. A.P., Russell, S.S., eds, Protostars & Planets IV. Univ. Arizona Press, Tuscon, p. 401
29. Igea, J., Glassgold, A.E., 1999, ApJ, 518, 848
30. Johns-Krull C.M., Valenti J.A., Linsky J.L., 2000, ApJ, 539, 815
31. Kenyon, S.J., Hartmann, L., 1995, ApJS, 101, 117
32. Krolik, J.H., Kallman, T.H., 1983, ApJ, 267, 610
33. Kurucz R.L., 1992, in Barbuy, B., Renzini, A., eds, Proc. IAU Symp. 149, Stellar Populations of Galaxies. Kluwer, Dordrecht, p. 225
34. Lada, C.J., Lada, E.A., 2003, ARA&A, 41, 57
35. Linsky, J.L., Wood, B.E., Judge, P., Brown, A., Andrulis, C., Ayres, T.R., 1995, ApJ, 442, 381
36. Linsky, J.L., Wood, B.E., Brown, A., Osten, R.A., 1998, ApJ, 492, 767
37. Mannings V., Sargent A.I., 1997, ApJ, 490, 792
38. Matsuyama I., Johnstone D., Hartmann L., 2003, ApJ, 582, 893
39. Najita, J., Carr, J.S., Mathieu, R.D., 2003, ApJ, 589, 931
40. Palla, F., Stahler, S.W., 2002, ApJ, 581, 1194
41. Persi, P., Marenzi, A.R., Olofsson, G. et al., 2000, A&A, 357, 219
42. Pringle, J.E., 1981, ARA&A, 19, 137
43. Richling S., Yorke, H.W., 1997, A&A, 327, 317
44. Shang, H., Glassgold, A.E., Shu, F.H., Lizano, S., 2002, ApJ, 564, 853
45. Simon, M., Prato, L., 1995, ApJ, 450, 824
46. Skrutskie, M. F., Dutkevitch, D., Strom, S.E., Edwards, S., Strom, K.M., Shure, M.A., 1990, AJ, 99, 1187
47. Wolk, S.J., Walter, F.M., 1996, AJ, 111, 2066